Nanodiamond for Hydrogen Storage: Temperature-dependent Hydrogenation and Charge-induced Dehydrogenation

Lin Lai,^{*a} **Amanda S. Barnard,**^{a‡}

Received Xth XXXXXXXXXX 20XX, Accepted Xth XXXXXXXXX 20XX
First published on the web Xth XXXXXXXXXX 200X
DOI: 10.1039/b000000x

1 Supplementary Information

1.1 Characterization of Nanodiamonds During Charge–Induced Dehydrogenation

As described int he main text, the adiabatic charging of the isolated hydrogenated C_{705} and C_{837} diamond nanoparticles were simulated by simply adding/removing electrons into/from the neutral systems and re-optimized the entire structures using the conjugate gradient scheme until the thermodynamically preferred structures are obtained. The charging and geometrical optimization was repeated until the mechanical failure was established, and the final structures were thoroughly characterised. The atomic configurations of five different states of the charged systems (labelled as *i*, *ii*, *iii*, *iv*, and *v*) are presented in figure 1, as well as in the main text. The labels *i*, *ii*, *iii*, *iv*, and *v* correspond to the vertical markers in Figure 2a, 2b, and 2c.

Figure 2 presents the characterisation of the structural integrity of the nanodiamonds throughout the process, in terms of the average C–H bond length ($R_{\mathrm{C-H}}$), C–C bond length ($R_{\mathrm{C-C}}$) and C–C–C bond angle ($\theta_{\mathrm{C-C-C}}$) here we can see that, even when the applied anionic or cationic charge is low, there is a consequential change in the structure of the nanodiamond as it accommodates the charge re-distribution. We can see the $R_{\mathrm{C-H}}$ increases along with the increase of the charges (figure 2a). As hydrogen is desorbed from the HNDs, the $R_{\mathrm{C-H}}$ is found to decrease accordingly until states *i* and *v*, where the $R_{\mathrm{C-H}}$ starts to notably fluctuate. The fluctuations of $R_{\mathrm{C-H}}$ are associated with the restructuring and changing hybridisation of the diamond surfaces beneath the remaining hydrogen atoms.

In addition to this the change of the average C–C bond length ($R_{\mathrm{C-C}}$) also remains relatively unchanged with the increase of the (either positive or negative) charges in HNDs, although the $R_{\mathrm{C-C}}$ enlarges with the increasing charges up to the states *ii* and *iv* (figure 2b). Further increasing the charges give rise to a slight decrease in $R_{\mathrm{C-C}}$ and a moderate fluctuation. From $R_{\mathrm{C-H}}$, the $R_{\mathrm{C-C}}$ exhibits great fluctuation, which is a sign of damage of the nanoparticles, until states *i* and *v*, where its value drastically drops. This is associated with the destruction of the nanoparticles, as seen via visual inspection of state *i* and *v* in figure 1. Figure 2c shows the average C–C–C angle (θ), as a function of charges per carbon, where again we found notable fluctuation in θ when charges exceed state *i* and *v*.

1.2 Characterization of Nanodiamonds with Partial or Anisotropic Hydrogenation

As mentioned in the main text, we have selectively and systematically patterned the two model structures with monolayers of hydrogen, with the hydrogen restricted *to* single facet types (i.e. just the $\{100\}$ facets, just the $\{111\}$ facets or just the $\{110\}$ facets) to enable a comparison of which facets may offer preferential sites for hydrogenation. In addition to this, adsorption was restricted *from* single facet types (i.e. all but the $\{100\}$ facets, all but the $\{111\}$ facets or all but the $\{110\}$ facets) to enable a comparison of which 'bare' facets may offer preferential reconstructions that increase the stability of the entire structure.

Fully relaxed structures of the both partly and entirely hydrogenated C_{705} and C_{837} diamonds nanoparticles are displayed in the main text, and the results of the coordination for C atoms and bond length for C–C and C–H are summarized in Table 1. We can see that H-$\{111\}$-termination induces a significant structural changes in both C_{705} and C_{837} nanodiamonds, which results in a dramatic increase in the fraction of sp^3-bonded C atoms, a decrease in the fraction of sp^{2+x}-bonded C atoms, and entirely absence of sp^2-bonded C atoms, compared with unsaturated nanodiamonds. It means surface hydrogenation converts the hybridization of C atoms from sp^2 to sp^3, breaks the reconstruction (graphitization) on the $\{111\}$ facets, and restores the 1×1 unreconstructed $\{111\}$ surface as on the crystalline diamond surface. This conclusion

---

^{a} *CSIRO Materials Science and Engineering, Clayton, VIC, 3168, Australia. Tel: +61 3 9545 7883; E-mail: lin.lai@csiro.au*

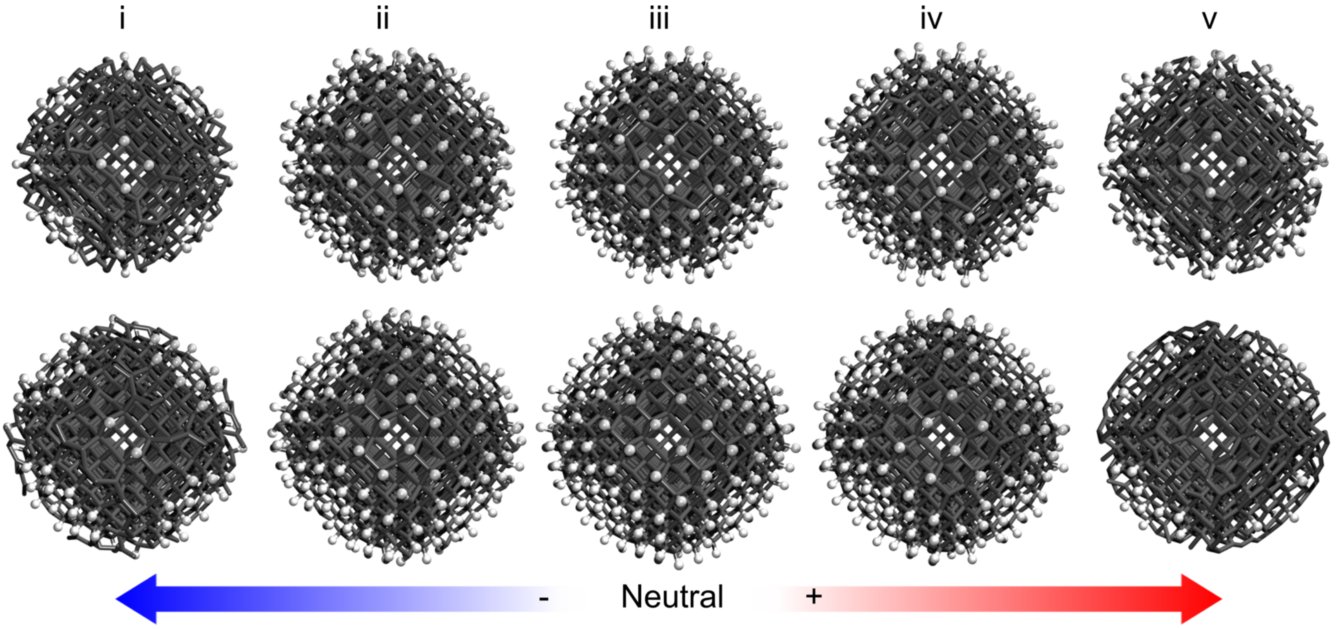

Fig. 1 Configurations of the State *i*, *ii*, *iii*, *iv*, and *v* of the C_{705} (upper) and C_{837} (bottom) diamond nanoparticles. Gray and red balls represent carbon and hydrogen atoms, respectively.

is supported by comparing the relaxed configurations of bare and H-{111}-terminated nanodiamonds (as shown in Figure 3). The average C–C bond length in H-{111}-terminated C_{705} and C_{837} nanodiamonds are $\sim 1.535 \pm 0.034$ Å and $\sim 1.538 \pm 0.026$ Å, respectively. Both of them are larger than that in bucky-diamond ($\sim 1.520 \pm 0.052$ Å), which implies the nanodiamond enlarges with H-{111}-passivation. The average C–H bond length is $\sim 1.117 \pm 0.001$ Å, a little larger than those in H-{100}-passivated and H-{110}-passivated nanodiamonds.

This is due to the higher density of the C–H bonds on the {111} facets. In contrast, the H-{100}-termination makes little changes in the fraction of sp^2-bonded C atoms, a slight increases in the fraction of sp^3-bonded C atoms, and a slight decrease in the fraction of the sp^{2+x}-bonded C atoms in the C_{705} nanodiamond. In the C_{837} nanodiamond, there is also a sight decrease in the fraction of sp^{2+x}-bonded C atoms, but the fraction of sp^3-bonded C atoms is almost unchanged with an increase in the fraction of sp^2-bonded C atoms. This difference is due to the lack of the {110} facets in the C_{837} nanodiamond. The H-{100}-termination have little impact on the graphitized {111} facets fully of sp^2-bonded C atoms with the {110} facets as a buffer in the C_{705} nanoparticle. However, the {100} facets share {100}—{111} edges with the {111} facets without any facets in the C_{837} nanoparticle. Consequently, the H-{100}-termination directly affects the bonding on the {111} facets and increases the fraction of sp^2-bonded C atoms. The C–C bond length is found to be nearly unchanged in the H-{100}-terminated nanoparticle, compared with the bare one, which suggests the H-passivation retains the 2 × 1 surface reconstruction of the {100} facets. The C–H bond length is $\sim 1.114 \pm 0.001$ Å and $\sim 1.115 \pm 0.002$ Å in the H-{100}-terminated C_{705} and C_{837} nanoparticles, respectively, which is smaller than those in the H-{111}-terminated and H-{110}-terminated nanoparticles.

The H-termination of the {110} facets induces a decease in the fraction of the sp^2-bonded C atoms, an increase in the fraction of the sp^3-bonded C atoms, and a slight decrease in the sp^{2+x}-bonded C atoms. This confirms our previous conclusion that the {110} facets, as a buffer, prevent the H-{100}-termination from affecting the bonding of the {111} facets. Here, the H-passivation of the "buffer" {110} facets indeed decrease the fraction of the sp^2-hybridized C atoms that belongs to the graphitized {111} facets. The average C–C bond length is $\sim 1.529 \pm 0.0474$ Å, larger than those of the bare and H-{100}-passivated nanoparticles and smaller than that of the H-{111}-passivated nanoparticle. The average C–H bond length is $\sim 1.114 \pm 0.001$ Å, which is similar to that in the H-{100}-passivation and smaller than that in the H-{111}-termination.

We find that the more H-termination in nanoparticle, the more fraction of sp^3-bonded C atoms. In the configuration of the C_{705} nanoparticle without {100}-, {110}-, and {111}-passivation (i.e. the {100} clean, {110} clean, and {111} clean, with 156, 168, and 132 C–H bonds, respectively), the fraction of sp^3-bonded C atoms is about 89.8%, 91.5%, and

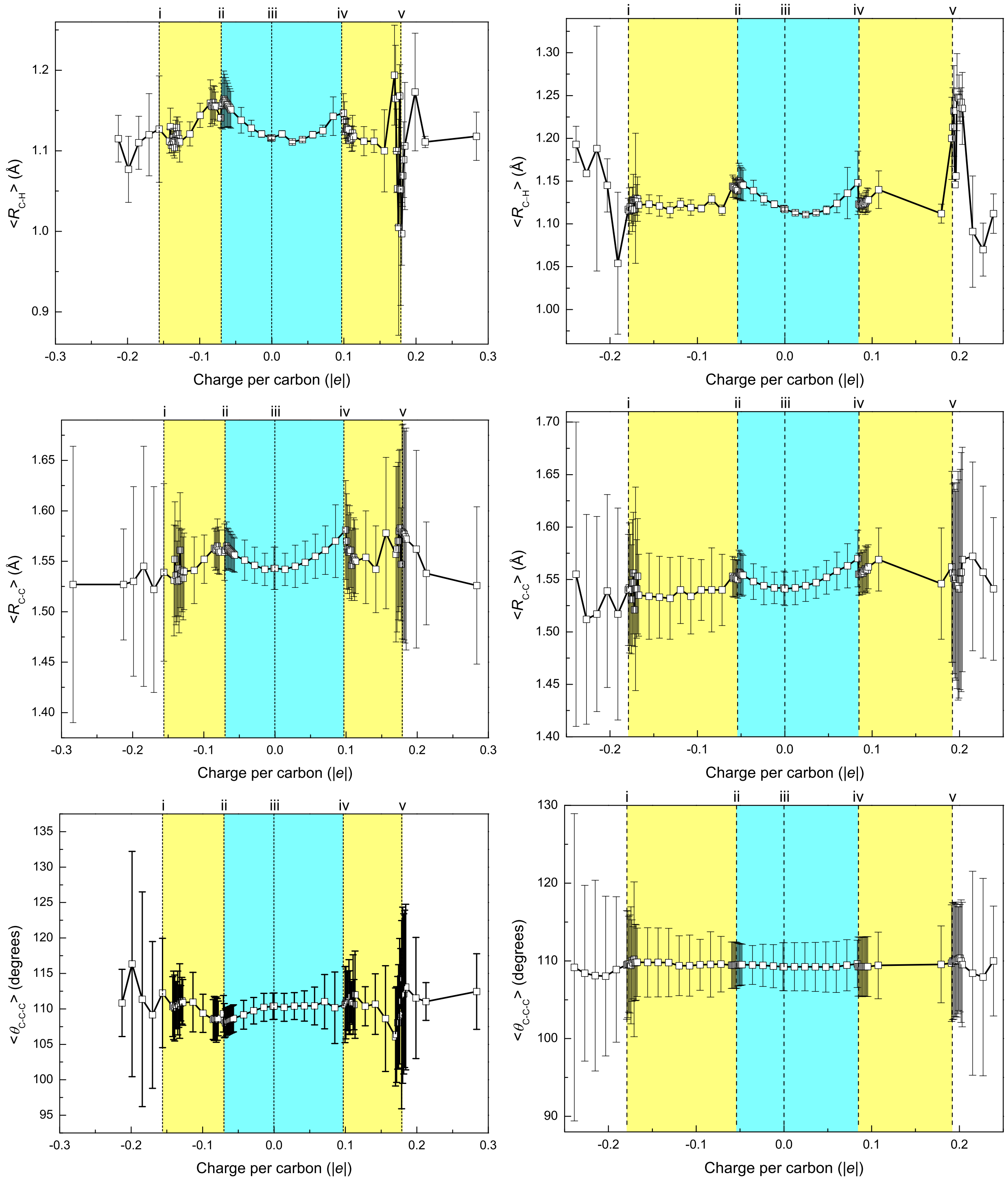

Fig. 2 Characterization of the fully hydrogenated C_{705} (left) and C_{837} (right) diamond nanoparticles as a function of charges per carbon. Shown is the average C–H bond length (upper panels), the average C–C bond length (centre panels) and the average C–C–C bond angle (lower panels). States *i*, *ii*, *iii*, *iv*, and *v* correspond to the structures present in Figure 1.

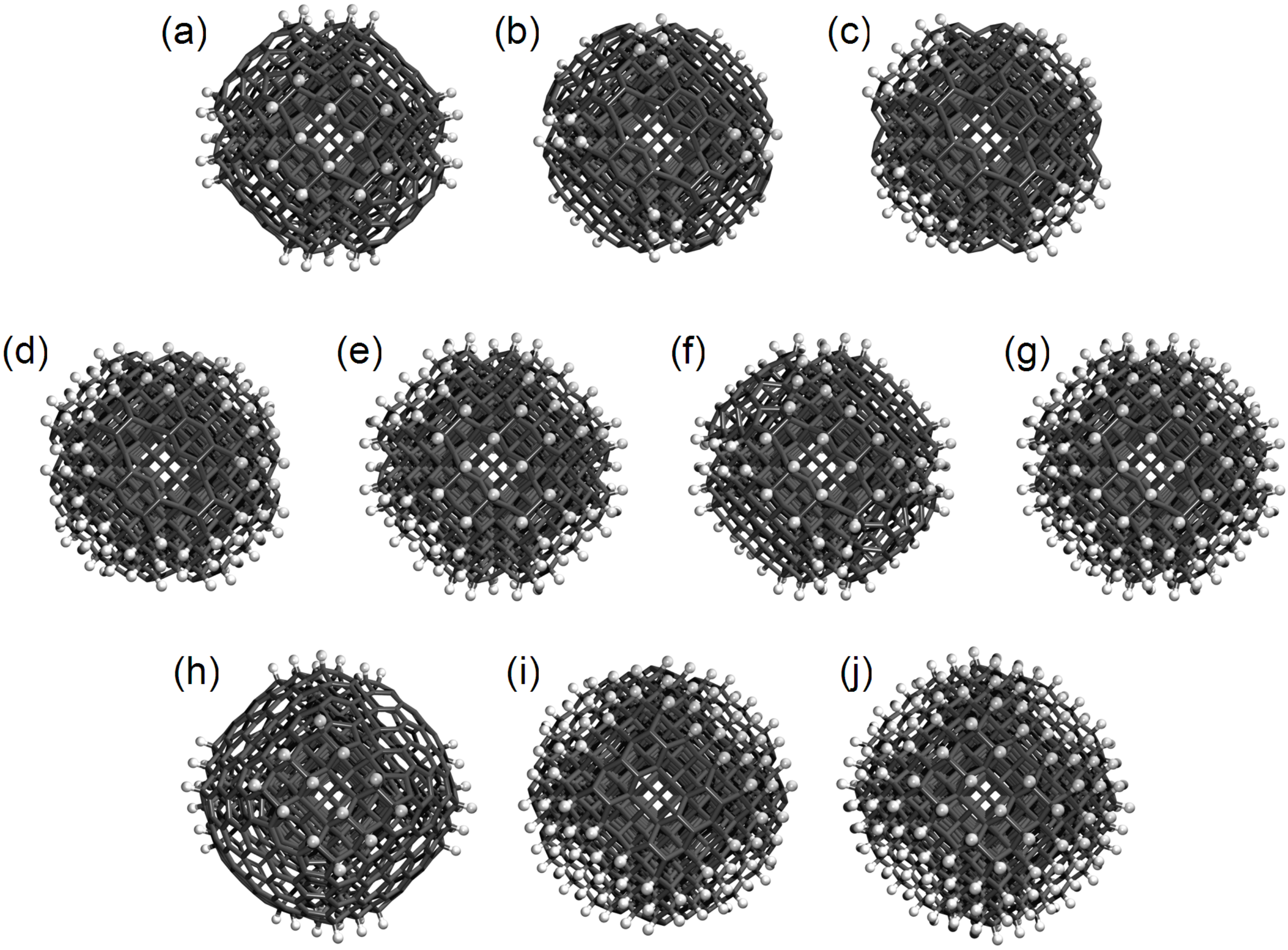

Fig. 3 Relaxed configurations of diamond nanoparticles with hydrogen functionalisation on all the (a) {100} facets, (b) {110} facets, (c) {111} facets, (d) {110}&{111} facets, (e) {100}&{111} facets, (f) {100}&{110} facets, and (g) entire surfaces of the C_{705} nanodiamond; and (h) {100} facets, (i) {111} facets, and (j) entire surfaces of the C_{837} nanodiamond. Red and gray balls represent hydrogen and carbon atoms, respectively.

Table 1 Fraction (%) of sp^1-, sp^2-, sp^3-, and sp^{2+x}-bonded C atoms and the average C–C and C–H bond lengths (Å) in the H-terminated C_{705} and C_{837} nanodiamonds.

Configurations	sp^1	sp^2	sp^3	sp^{2+x}	C–C	C–H
C_{705} bare	0.0	19.3	52.9	27.8	1.520 ± 0.060	-
C_{705} (100)-passivation	0.0	20.1	63.1	16.7	1.520 ± 0.052	1.114 ± 0.001
C_{705} (110)-passivation	0.0	7.9	68.5	23.5	1.529 ± 0.047	1.114 ± 0.001
C_{705} (111)-passivation	0.0	0.0	81.3	18.7	1.535 ± 0.034	1.117 ± 0.001
C_{705} (100) clean	0.0	0.0	89.8	10.2	1.539 ± 0.029	1.116 ± 0.002
C_{705} (110) clean	0.0	0.0	91.5	8.5	1.540 ± 0.027	1.116 ± 0.002
C_{705} (111) clean	0.0	3.4	83.3	13.3	1.538 ± 0.049	1.114 ± 0.002
C_{705} full-passivation	0.0	0.0	100.0	0.0	1.543 ± 0.021	1.116 ± 0.002
C_{837} bare	0.0	33.0	37.4	29.6	1.500 ± 0.060	-
C_{837} (100)-passivation	0.0	46.6	39.1	14.3	1.498 ± 0.057	1.115 ± 0.002
C_{837} (111)-passivation	0.0	0.0	91.4	8.6	1.538 ± 0.026	1.118 ± 0.001
C_{837} full-passivation	0.0	0.0	100.0	0.0	1.541 ± 0.016	1.117 ± 0.002

83.3%, respectively. Naturally, the fraction of the sp^2- and sp^{2+x}-bonded C atoms decreases in these configurations. In the full-H-terminated nanoparticles, all the C atoms are sp^3-hybridized.

In addition, we find the average C–C bond length increases due to the hydrogenation. The full-H-termination leads to similar average C–C bond length, about 1.543 ± 0.021 Å and 1.541 ± 0.016 Å for the C_{705} and C_{837} nanoparticles, respectively. However, they are about 1.520 ± 0.060 Å and 1.500 ± 0.060 Å in the bare C_{705} and C_{837} nanoparticles, respectively. The average C–H bond length is also increased in these configurations. The only exception is the configuration of the H-$\{111\}$-clean, in which the average C–H bond length is $\sim 1.114 \pm 0.002$ Å due to the absence of C–H bonds of the $\{111\}$ facets.

Acknowledgement

Computational resources for this project have been supplied by the National Computing Infrastructure (NCI) national facility under MAS Grant q27.